

Superlight Small Bipolarons in the Presence of a Strong Coulomb Repulsion

J. P. Hague,¹ P. E. Kornilovitch,² J. H. Samson,¹ and A. S. Alexandrov¹

¹*Department of Physics, Loughborough University, Loughborough, LE11 3TU, United Kingdom*

²*Hewlett-Packard Company, 1000 Nebraska Circle Blvd, Corvallis, Oregon 97330, USA*

(Received 1 June 2006; published 16 January 2007)

We study a lattice bipolaron on a staggered triangular ladder and triangular and hexagonal lattices with both long-range electron-phonon interaction and strong Coulomb repulsion using a novel continuous-time quantum Monte Carlo algorithm to solve the two-particle Coulomb-Fröhlich model. The algorithm is preceded by an exact integration over phonon degrees of freedom, and as such is extremely efficient. The bipolaron effective mass and radius are computed. Bipolarons on lattices constructed from triangular plaquettes have a novel crablike motion, and are small but very light over a wide range of parameters. We discuss the conditions under which such particles may form a Bose-Einstein condensate with high transition temperature, proposing a route to room temperature superconductivity.

DOI: [10.1103/PhysRevLett.98.037002](https://doi.org/10.1103/PhysRevLett.98.037002)

PACS numbers: 74.20.Mn, 71.38.-k

As recognized by Landau, Pekar, and Fröhlich, an electron may drag a lattice distortion as it moves through an ionic material, leading to a new particle—the polaron, which has quite different properties from the original electron (for reviews see, for example, Refs. [1,2]). At weak coupling, two polarons can be bound into a large bipolaron via exchange forces, without assuming anything more complicated than the Fröhlich electron-phonon interaction (EPI) [3]. On increasing density large bipolarons overlap, giving rise to either a conventional (BCS) superconductor or a normal metal. At strong coupling, the EPI may overcome the Coulomb repulsion between electrons, so the resulting interaction becomes attractive at a distance of the order of the lattice constant [4] and two small polarons form tightly bound pairs, i.e., small bipolarons. Earlier studies [5] considered small bipolarons as localized objects. However, a perturbation expansion in terms of hopping integrals has proved they are itinerant quasiparticles existing in Bloch states and forming a Bose-Einstein condensate (BEC) of charge $2e$ bosons at low temperatures [6].

For very strong EPI, polarons are “self-trapped” on a single lattice site, with energy $E_p = -\lambda z t$, where λ is the electron-phonon coupling constant, t is the hopping parameter and z is the coordination number. Expanding about the atomic limit in small t (which is small compared to E_p in the small polaron regime, $\lambda > 1$) the polaron mass is computed as $m^* = m_0 \exp(\gamma z t \lambda / \hbar \omega)$, where ω is the frequency of Einstein phonons, m_0 is the rigid lattice band mass, and γ is a numerical constant. For the Holstein model [7], which is purely site local, $\gamma = 1$. Bipolarons are on-site singlets in the Holstein model and their mass m_H^{**} appears only in the second order of t [6] scaling as $m_H^{**} \propto (m^*)^2$ in the limit $\hbar \omega \gg \Delta$, and as $m_H^{**} \propto (m^*)^4$ in a more realistic regime $\hbar \omega \ll \Delta$ [4]. Here $\Delta = 2E_p - U$ is the bipolaron binding energy, and U is the on-site (Hubbard) repulsion. Since the Hubbard U is 1 eV or larger

in strongly correlated materials, the EPI must be large to stabilize on-site bipolarons and the Holstein bipolaron mass appears very large, $m_H^{**}/m_0 > 1000$, for realistic values of phonon frequency.

This estimate led some authors to the conclusion that the formation of itinerant small polarons and bipolarons in real materials is unlikely [8], and high-temperature bipolaronic superconductivity is impossible [9]. However, one should note that the Holstein model is an extreme polaron model, and typically yields the highest possible value of the (bi)-polaron mass in the strong-coupling limit. Many advanced materials with low density of free carriers and poor mobility (at least in one direction) are characterized by poor screening of high-frequency optical phonons and are more appropriately described by a long-range Fröhlich EPI [4]. For Fröhlich type interactions, the parameter $\gamma < 1$ ($\gamma \approx 0.3$ on square and triangular lattices [10,11]), reflecting the fact that when an electron hops the lattice is already partially deformed. Thus, the unscreened Fröhlich EPI forms relatively light small polarons, which are several orders of magnitude lighter than small Holstein polarons. This has been confirmed numerically by Monte Carlo simulations [11,12], Lanczos diagonalization [13], and variational calculations [14].

This unscreened Fröhlich interaction combined with on-site repulsive correlations can also bind holes into mobile intersite bipolarons [10,15]. Using an advanced variational method, Bonča and Trugman [14] studied the binding of two electrons via the chain model of Ref. [12] with nearest-neighbor EPI and a Hubbard U . Intersite bipolarons of Ref. [14] propagate along the chain with a light mass which is, however, still second order in the polaron mass as in the Holstein model.

Here we study a bipolaron on a staggered triangular ladder (1D), triangular (2D), and strongly anisotropic hexagonal (3D) lattices using a continuous-time quantum Monte Carlo technique. On such lattices, bipolarons are found to move with a crablike motion [Fig. 1(b)], which is

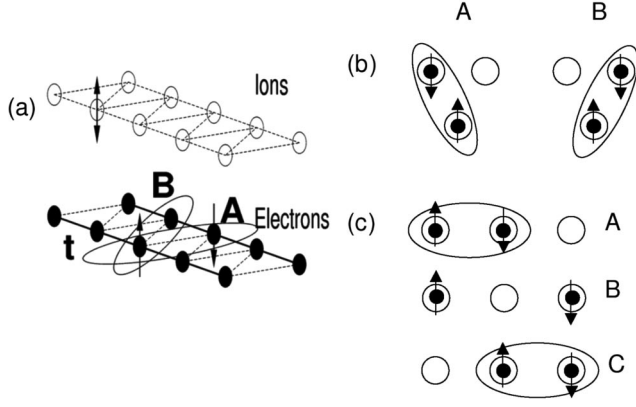


FIG. 1. (a) Schematic of the ladder model. Electrons sit on opposite sides (legs) of a staggered ladder with intersite distance a , with ions vibrating across the ladder on an identical system sitting a height a above the electron legs. (b) Schematic motion of the crab bipolaron—states A and B are degenerate. (c) Schematic of the crawler motion.

distinct from the crawler motion [Fig. 1(c)] on cubic lattices [6,14]. Such bipolarons are both small and very light (first order in the polaron mass) for a wide range of electron-phonon couplings and phonon frequencies.

We use a generic Coulomb-Fröhlich model of electron-phonon interactions in layered 2D materials which has the following Hamiltonian,

$$H = -t \sum_{\langle \mathbf{nn}' \rangle \sigma} c_{\mathbf{n}'\sigma}^\dagger c_{\mathbf{n}\sigma} + \frac{1}{2} \sum_{\mathbf{nn}'\sigma\sigma'} V(\mathbf{n}, \mathbf{n}') c_{\mathbf{n}\sigma}^\dagger c_{\mathbf{n}\sigma} c_{\mathbf{n}'\sigma'}^\dagger c_{\mathbf{n}'\sigma'} + \sum_{\mathbf{m}} \frac{\hat{p}_{\mathbf{m}}^2}{2M} + \sum_{\mathbf{m}} \frac{\xi_{\mathbf{m}}^2 M \omega^2}{2} - \sum_{\mathbf{nm}\sigma} f_{\mathbf{m}}(\mathbf{n}) c_{\mathbf{n}\sigma}^\dagger c_{\mathbf{n}\sigma} \xi_{\mathbf{m}}. \quad (1)$$

Each vibrating ion has one phonon degree of freedom $\xi_{\mathbf{m}}$ associated with a single atom. The sites are numbered by the indices \mathbf{n} or \mathbf{m} for electrons and ions, respectively. Operators c annihilate electrons. The phonon subsystem is a set of independent oscillators with frequency ω and mass M . Here $\langle \mathbf{nn}' \rangle$ denote pairs of nearest neighbors, and $\hat{P}_{\mathbf{m}} = -i\hbar \partial / \partial \xi_{\mathbf{m}}$ is the ion momentum operator. In the plane electrons are mobile, and hence in-plane instantaneous

Coulomb repulsion $V(\mathbf{n}, \mathbf{n}')$ is heavily screened, with only on-site repulsion U and nearest-neighbor repulsion V_C . In contrast, the Fröhlich interaction is assumed to be long range, due to unscreened interaction with c -axis high-frequency phonons [4]. The form of the interaction with c -axis polarized phonons is specified via the force function [12], $f_{\mathbf{m}}(\mathbf{n}) = \kappa [(\mathbf{m} - \mathbf{n})^2 + 1]^{-3/2}$, where κ is a constant. The dimensionless electron-phonon coupling constant λ is defined as $\lambda = \sum_{\mathbf{m}} f_{\mathbf{m}}^2(0) / 2M\omega^2 zt$, which is the ratio of the polaron energy at $t = 0$ to the kinetic energy of the free electron zt . Following the same argument that was used to justify the in-plane long-range Fröhlich interaction, the Coulomb interaction between electrons in neighboring planes is not well screened, as discussed later in this Letter.

In the limit of high phonon frequency $\hbar\omega \gg t$ and large on-site Coulomb repulsion, the model is reduced to an extended Hubbard model with intersite attraction and suppressed double occupancy [15]. Then the Hamiltonian can be projected onto the subspace of nearest-neighbor intersite crab bipolarons. In contrast with the crawler bipolaron, the crab bipolaron's mass scales linearly with the polaron mass ($m^{**} = 4m^*$ on the staggered chain and $m^{**} = 6m^*$ on the triangular lattice). Here, we aim to determine if such a bipolaron can exist for realistic values of the electron-phonon coupling and phonon frequency.

To answer this question, we have extended the continuous-time quantum Monte-Carlo (CTQMC) algorithm [11,12,16,17] to systems of two particles with long-range EPI and strong Coulomb repulsion. We have solved the bipolaron problem on a staggered ladder [Fig. 1(a)] and on triangular and anisotropic hexagonal lattices from weak to strong coupling in a realistic parameter range where usual limiting approximations fail. The CTQMC method employed here has been described in detail with regard to the single polaron problem in Refs. [11,16,17]. Here we give a quick overview of the extended algorithm. The initial step is to determine the effective bipolaron action that results when the phonon degrees of freedom have been integrated out analytically. The action is a functional of two polaron paths in imaginary time which form the bipolaron and is given by the following double integral,

$$A[\mathbf{r}(\tau), \mathbf{r}(\tau')] = \frac{z\lambda\bar{\omega}}{2\Phi_0(0,0)} \int_0^{\bar{\beta}} \int_0^{\bar{\beta}} d\tau d\tau' e^{-\bar{\omega}\bar{\beta}/2} (e^{\bar{\omega}(\bar{\beta}/2 - |\tau - \tau'|)} + e^{-\bar{\omega}(\bar{\beta}/2 - |\tau - \tau'|)}) \sum_{ij} \Phi_0(\mathbf{r}_i(\tau), \mathbf{r}_j(\tau')) + \frac{z\lambda\bar{\omega}}{\Phi_0(0,0)} \times \int_0^{\bar{\beta}} \int_0^{\bar{\beta}} d\tau d\tau' e^{-\bar{\omega}\tau} e^{-\bar{\omega}(\bar{\beta} - \tau')} \sum_{ij} [\Phi_{\Delta\mathbf{r}}(\mathbf{r}_i(\tau), \mathbf{r}_j(\tau')) - \Phi_0(\mathbf{r}_i(\tau), \mathbf{r}_j(\tau'))] - \int_0^{\bar{\beta}} \frac{V(\mathbf{r}_1(\tau), \mathbf{r}_2(\tau))}{2} d\tau. \quad (2)$$

The full interaction between the particles is $\Phi_{\Delta\mathbf{r}}(\mathbf{r}(\tau), \mathbf{r}(\tau')) = \sum_{\mathbf{m}} f_{\mathbf{m}}(\mathbf{r}(\tau)) f_{\mathbf{m} + \Delta\mathbf{r}}(\mathbf{r}(\tau'))$. $\bar{\omega} = \hbar\omega/t$ and $\bar{\beta} = t/k_B T$, with $\bar{\beta} \gg (\hbar\omega)^{-1}$. The ends of the two paths at $\tau = 0$ and $\tau = \bar{\beta}$ are related by an arbitrary translation, $\Delta\mathbf{r}$. The indices $i = 1, 2$ and $j = 1, 2$ represent the fermion paths. Analytic integration is performed over sec-

tions of parallel paths. From this starting point, the bipolaron is simulated using the Metropolis Monte Carlo (MC) method. The electron paths are continuous in time with hopping events (or kinks) introduced or removed from the path with each MC step. In contrast to the one-particle case, fixing the end configurations limits the update pro-

cedure to inserting and removing pairs of kinks and antikinks (kinks facing in the opposite direction). We have identified 8 different types of such binary updates which can be used in the Monte Carlo procedure. We also exchange the paths using a combination of kink insertion and antikink removal, and using some of the binary updates. From the ensemble, the ground state bipolaron energy and effective mass are computed as in Ref. [16]. The bipolaron radius is computed as

$$R_{\text{bp}} = \left\langle \sqrt{\frac{1}{\beta} \int_0^\beta \Delta \mathbf{r}_{12}(\tau)^2 d\tau} \right\rangle. \quad (3)$$

Figure 2(a) shows the ratio of polaron to bipolaron masses on the staggered ladder as a function of effective coupling and phonon frequency for $V_C = 0$. The bipolaron to polaron mass ratio is about 2 in the weak coupling regime ($\lambda \ll 1$) as it should be for a large bipolaron [3]. In the strong coupling, large phonon frequency limit the mass ratio approaches 4, in agreement with arguments given above. In a wide region of parameter space, we find a bipolaron/polaron mass ratio of between 2 and 4 and a bipolaron radius similar to the lattice spacing, see Figs. 2(b) and 3. Thus the bipolaron is small and light at the same time. Taking into account additional intersite Coulomb repulsion V_C does not change this conclusion. The bipolaron is stable for $V_C < 4t$, see inset of Fig. 3. As V_C increases the bipolaron mass decreases but the radius remains small, at about 2 lattice spacings. Significantly, the

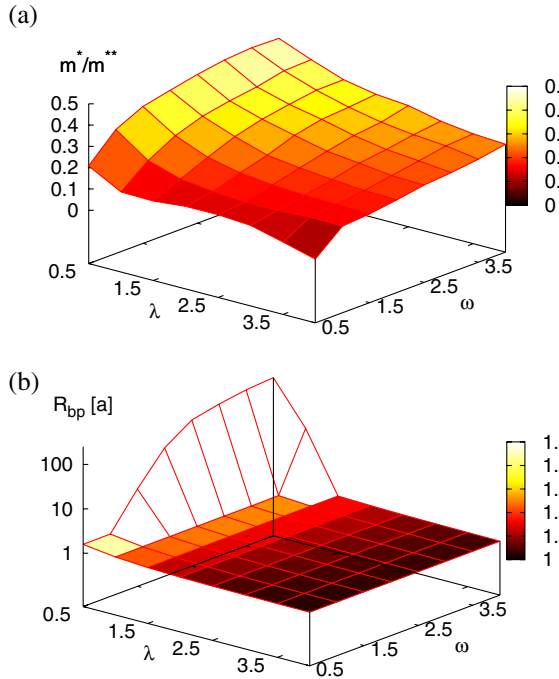


FIG. 2 (color online). Staggered ladder. (a) Polaron to bipolaron mass ratio for a range of $\bar{\omega}$ and λ . (b) Bipolaron radius. Mobile small bipolarons are seen in the adiabatic regime $\bar{\omega} = 0.5$ for couplings λ up to 2.5.

absolute value of the small bipolaron mass is only about 4 times the bare electron mass m_0 , for $\lambda = \hbar\omega/t = 1$ (see Fig. 3).

The toy problem on the triangular ladder contains the essential physics of the crab bipolaron. We demonstrate this by simulating the bipolaron on an infinite triangular lattice including exchanges and large on-site Hubbard repulsion $U = 20t$ and $V_C = 0$ (Fig. 4). Moderate couplings at $\hbar\omega = t$ also lead to light small bipolarons. Finally, we have simulated the bipolaron on a hexagonal lattice, with out-of-plane hopping $t' = 0.3t$, and a short range phonon-mediated interplane interaction [$\Phi_h(n, n') = \Phi_l(n, n')\delta_{r,r'}$ where r are plane indices, subscript h stands for hexagonal and l for triangular]. We have calculated values of the bipolaron mass and radius for experimentally achievable values of the phonon frequency $\hbar\omega = t = 200$ meV and electron-phonon coupling $\lambda = 0.36$. We have found a light in-plane mass, $m_{xy}^{**} = (4.49 \pm 0.04)m_{0xy}$. Out-of-plane $m_z^{**} = (68.4 \pm 1)m_{0z}$ is Holstein-like, where $m_{0z} = \hbar^2/2d^2t'$ and $m_{0xy} = \hbar^2/3a^2t$. The bipolaron radius is $R_{\text{bp}} = (2.60 \pm 0.03)a$, sitting mainly in the xy plane. Comparison with Fig. 4 shows that the z -axis Holstein interaction generates a very effective potential barrier, maintaining the quasiparticle in the plane, and ensuring its stability as interplane hopping is introduced. Since the particle is well localized in the z direction, the residual Coulomb interplane repulsion will also act to enhance the in-plane pairing.

We now discuss the possible condensation of such quasiparticles. When bipolarons are small and pairs do not overlap, the pairs can form a BEC at $k_B T_{\text{BEC}} = 3.31\hbar^2(2n_B/a^2\sqrt{3}d)^{2/3}/(m_{xy}^{**2/3}m_z^{**1/3})$. If we choose realistic values for the lattice constants of 0.4 nm in the plane and 0.8 nm out of the plane, and allow the density of bosons to be $n_B = 0.12$ per lattice site, which easily avoids overlap of pairs, then $T_{\text{BEC}} = 323$ K. There are several situ-

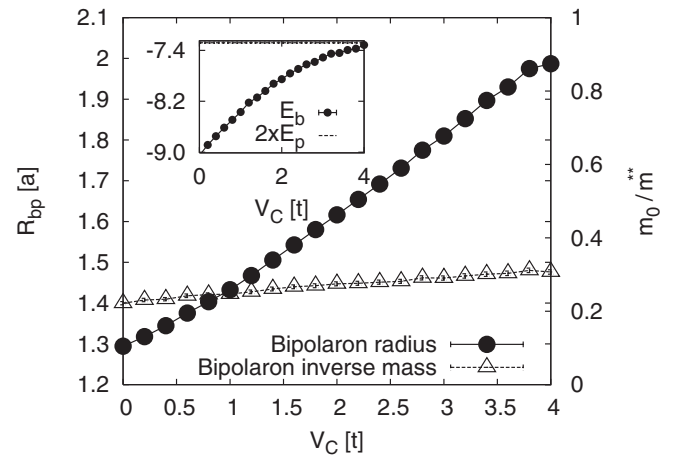


FIG. 3. Variation of bipolaron energy, mass, and radius (in units of a) as intersite Coulomb repulsion V_C is increased for λ and $\bar{\omega} = 1$ on the staggered ladder.

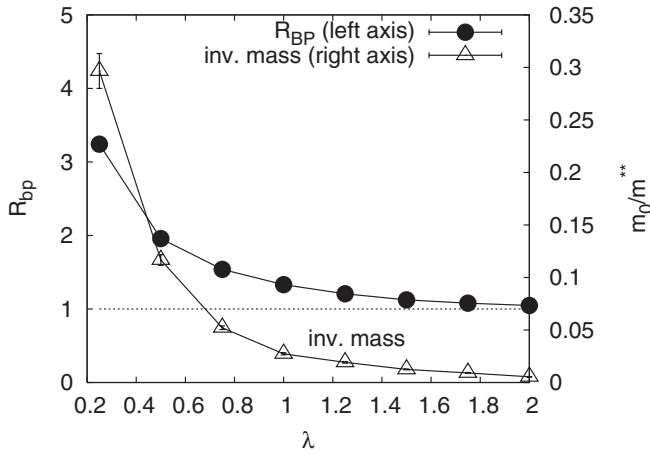


FIG. 4. Variation of bipolaron mass and radius for various λ , with $\bar{\omega} = 1$ on a triangular lattice. Small, light bipolarons (as shown here) are a necessary precursor to high-temperature BEC, and are superlight compared to Holstein bipolarons.

ations under which a BEC might not be formed. The long-range nature of the Fröhlich interaction might cause clustering of polarons into finite-size mesoscopic textures, destroying the condensate. However, the long-range inter-plane repulsion between bipolarons will stop bipolarons from pairing, as long as there is a sufficiently large density of particles. The analytical analysis of such multipolaron systems in the antiadiabatic limit on the ladder and on a two-dimensional lattice [15] agrees with this argument, revealing a window in the parameter space where small bipolarons are formed while n -particle bound states with $n \geq 3$ do not exist. Furthermore, Monte Carlo studies of mesoscopic textures with realistic lattice deformations and Coulomb repulsion [18] show that bipolarons also dominate over phase separation in the adiabatic limit since they effectively repel each other [1].

Also, long-range Coulomb repulsion might in principle cause Wigner crystallization of the (bi)polaronic liquid. However, in highly polarizable ionic lattices with a large static dielectric constant, $\epsilon_0 \gg 1$, where the Coulomb-Fröhlich model is relevant, the net long-range repulsion is relatively weak since the relevant dimensionless parameter $r_s = m^* e^2 / \epsilon_0 (4\pi x / 3a^2 d)^{1/3} \lesssim 1$ at any relevant density and effective mass. The Wigner crystallization appears around $r_s \approx 100$ or larger, which corresponds to an extremely small atomic density of (bi)polarons $x \leq 10^{-6}$ when $\epsilon_0 = 30$ (like in $\text{La}_{2-x}\text{Sr}_x\text{CuO}_4$) and $m^* = 5m_e$. Hence, we expect the (bi)polaronic carriers to be in the liquid state at relevant doping levels, as required. A small value of r_s is also important so that there is a negligible correction to T_{BEC} due to the long-range interaction between bipolarons. r_s is expected to be small in ionic materials, which justifies our estimate assuming free bipolarons.

In summary, the CTQMC algorithm has been extended to simulate bipolarons formed in the Coulomb-Fröhlich model, leading to an unusual configuration on triangular lattices that is both small and superlight (especially compared to Holstein bipolarons). Such a particle has been found in a wide parameter range using CTQMC at achievable phonon frequencies and couplings in the presence of strong Coulomb repulsion. Such bipolarons might have a superconducting transition in excess of room temperature. We believe that the following recipe is worth investigating: (a) The parent compound should be an ionic insulator with light ions to form high-frequency optical phonons. (b) The structure should be quasi two-dimensional to ensure poor screening of high-frequency c -axis polarized phonons, but good in-plane screening. (c) A triangular lattice is required in combination with strong, on-site Coulomb repulsion to form the small superlight crab bipolaron.

The authors acknowledge support from EPSRC (UK) grants No. EP/C518365/1 and No. EP/D07777X/1, and useful discussions with J. Devreese, P. Edwards, V. Kabanov, Y. Liang, M. Stoneham, and P. Zhao.

-
- [1] A. S. Alexandrov and N.F. Mott, Rep. Prog. Phys. **57**, 1197 (1994).
 - [2] J. T. Devreese, in *Encyclopedia of Physics* (Wiley-VHC, Berlin, 2005).
 - [3] G. Verbist, F. M. Peeters, and J. T. Devreese, Phys. Rev. B **43**, 2712 (1991).
 - [4] A. S. Alexandrov, *Theory of Superconductivity: From Weak to Strong Coupling* (IOP, Bristol, 2003).
 - [5] P. W. Anderson, Phys. Rev. Lett. **34**, 953 (1975).
 - [6] A. S. Alexandrov and J. Ranninger, Phys. Rev. B **23**, 1796 (1981).
 - [7] T. Holstein, Ann. Phys. (N.Y.) **8**, 325 (1959); **8**, 343 (1959).
 - [8] E. V. L. de Mello and J. Ranninger, Phys. Rev. B **58**, 9098 (1998).
 - [9] P. W. Anderson, *The Theory of Superconductivity in the Cuprates* (Princeton University, Princeton NY, 1997).
 - [10] A. S. Alexandrov, Phys. Rev. B **53**, 2863 (1996).
 - [11] J. P. Hague *et al.*, Phys. Rev. B **73**, 054303 (2006).
 - [12] A. S. Alexandrov and P. E. Kornilovitch, Phys. Rev. Lett. **82**, 807 (1999).
 - [13] H. Fehske, J. Loos, and G. Wellein, Phys. Rev. B **61**, 8016 (2000).
 - [14] J. Bonča and S. A. Trugman, Phys. Rev. B **64**, 094507 (2001).
 - [15] A. S. Alexandrov and P. E. Kornilovitch, J. Phys. Condens. Matter **14**, 5337 (2002).
 - [16] P. E. Kornilovitch, Phys. Rev. Lett. **81**, 5382 (1998); Phys. Rev. B **60**, 3237 (1999).
 - [17] P. E. Spencer *et al.*, Phys. Rev. B **71**, 184310 (2005).
 - [18] T. Mertelj, V. V. Kabanov, and D. Mihailovic, Phys. Rev. Lett. **94**, 147003 (2005).